Original Article

J Vet Sci 2017, 18(4), 531-540 · https://doi.org/10.4142/jvs.2017.18.4.531

JVS

Molecular cloning and characterization of porcine ribosomal protein L21

Wu-Sheng Sun[1,2], Ju-Lan Chun[2], Dong-Hwan Kim[1], Jin-Seop Ahn[1], Min-Kyu Kim[2], In-Sul Hwang[3], Dae-Jin Kwon[3], Seongsoo Hwang[3,*], Jeong-Woong Lee[1,*]

[1]*Biotherapeutics Translational Research Center, Korea Research Institute of Bioscience and Biotechnology, Daejeon 34141, Korea*
[2]*Department of Animal Science and Biotechnology, College of Agriculture and Life Science, Chungnam National University, Daejeon 34134, Korea*
[3]*Animal Biotechnology Division, National Institute of Animal Science, Wanju 55365, Korea*

Ribosomal protein L21 (RPL21) is a structural component of the 60S subunit of the eukaryotic ribosome. This protein has an important role in protein synthesis and the occurrence of hereditary diseases. Pig is a common laboratory model, however, to the best of our knowledge, its *RPL21* gene has not been cloned to date. In this study, we cloned and identified the full-length sequence of the pig *RPL21* gene for the first time. In addition, we examined its expression pattern and function by using overexpression or knockdown approaches. As a result, we obtained a 604 bp segment that contains a 483 bp open reading frame encoding 160 amino acids. The pig *RPL21* gene is located in the "+" strand of chromosome 11, which spans 2167 bp from 4199792 to 4201958. Pig *RPL21* protein has nine strands and two helices in its secondary structure. Pig *RPL21* is predominantly expressed in ovary and lung, at lower levels in kidney, small intestine, and skin, and at the lowest levels in heart and liver. Furthermore, *RPL21* expression is closely connected with cell proliferation and cell cycle arrest. The results are intended to provide useful information for the further study of pig *RPL21*.

Keywords: *Sus scrofa*, conservation, gene expression, molecular cloning, ribosomal protein L21

Introduction

Ribosomes are important organelles involved in protein synthesis. Eukaryotic ribosomes are composed of a small subunit (40S) and a large subunit (60S) that together form an 80S ribosome [43]. Both of these subunits include complexes of different types of rRNAs and ribosomal proteins (RP). There are now at least 80 RPs reported in mammals [22,41] and 53 in *Escherichia coli* [40] that have been identified as part of a large ribosomal subunit. Additionally, these RPs are not only involved in regulating DNA transcription, DNA replication, DNA repair, and RNA splicing and modification [11], but they also have extraribosomal roles in regulating cell growth and metabolism [21,38,39].

Ribosomal protein L21 (RPL21) is an RP with a homologous counterpart in archaea (RPL21e) and with a functional analog in bacteria (RPL27). Archaeal RPL21e is bound in a similar ribosomal location as that of bacterial RPL27 [10,16]. The human *RPL21* gene maps to chromosome 13q12.2 [46] and encodes a 160 amino acid protein. It is reported that *RPL21* is involved in embryogenesis [23,37], odontogenesis [42], and age-related cataracts in human [3,44]. More importantly, the *RPL21* gene is considered to be the main cause of hypotrichosis simplex, a type of sustained hair loss occurring from early childhood to adulthood [46]. Therefore, more research into this gene is needed, but not only in humans. Pig, *Sus scrofa*, is a common laboratory model, however, to the best of our knowledge, its *RPL21* gene has not been characterized in research published to date. In this study, we cloned and identified the full-length sequence of the pig *RPL21* gene for the first time. We have also predicted its corresponding amino acid sequence and spatial structure. In addition, we analyzed the mRNA expression and molecular functions of *RPL21*. These results should provide a basis for further studies of the pig *RPL21* gene and hypotrichosis simplex.

Received 13 May 2016, Revised 12 Oct. 2016, Accepted 23 Nov. 2016
*Corresponding authors: Tel: +82-42-860-4428; Fax: +82-42-860-4608; E-mails: jwlee@kribb.re.kr (JW Lee), hwangss@korea.kr (S Hwang)
pISSN 1229-845X
eISSN 1976-555X

Materials and Methods

Total RNA extraction and 5′/3′ rapid amplification of cDNA ends (RACE) polymerase chain reaction (PCR)

Pig tissues were collected from a 3-month-old female Korean native pig. The animal procedures were approved by the Institutional Animal Care and Use Committee of the National Institute of Animal Science, Rural Development Administration (RDA) (approval No. NIAS2015-671). Total RNA was isolated from the different samples by using Trizol reagent (Invitrogen, USA) according to the manufacturer's protocol. The 5′ RACE was performed by using a 5′/3′ RACE kit (Roche Applied Science, Switzerland) and a variety of primers (Table 1). Briefly, first-strand cDNA was synthesized from total RNA extracted from the lung using primer 1. The first PCR was performed by using primers 2 and 3, with the A-tailed first-strand cDNA as a template. The nested PCR was performed by using primers 4 and 5 with the first PCR product diluted 1/20 as a template. The fragment obtained from 5′ RACE was subsequently cloned and sequenced. Similarly, 3′ RACE was performed by using the SMARTer RACE cDNA Amplification kit (Clontech, Japan). Primer 6 was used for synthesizing the first-strand cDNA, and a mix of primers 7 and 8 was used for the PCR reaction.

Characterization and annotation of the porcine *RPL21* gene

The open reading frames (ORFs) from the cloned mRNAs were predicted by using the translate tool in ExPaSy [2]. Multiple sequence alignment was performed by using Clustal X 1.83 [5]. An evolutionary tree was constructed by using MEGA5.1 [33] with the neighbor-joining method and 1,000 bootstrap runs. InterProScan software ver. 5 [13] was used to analyze the secondary structure, protein domain motifs, and for recognition of families of *RPL21*. N-glycosylation sites were predicted by using NetNGlyc 1.0 (Center for Biological Sequence Analysis, Denmark). Protein structure modeling was conducted by using SWISS-MODEL workspace with modeler 1vx4.1.T [14] as a template. The amino acid sequences of the RPL21 protein from 13 other species that were used in constructing phylogenetic trees were obtained from the National Center for Biotechnology Information (USA). In addition to our real-time PCR data for pig, we also used data from a public gene expression database in BioGPS. The raw data for human *RPL21* expression was extracted from probe sets 20012 at in the GeneAtlas U133A

Table 1. Oligonucleotide primers used in this study

Primer	Nucleotide sequence (5′-3′)	Primer length (bp)	Application
Primer 1	GCCAAGTGCTCCACCCGTAGCCA	24	cDNA synthesis
Primer 2	GACCACGCGTATCGATGTCGACTTTTTTTTTTTTTTTV	39	5′ RACE; outer
Primer 3	TGAAGTGCTGCTCTGCTGTCTCC	23	5′ RACE; outer
Primer 4	GACCACGCGTATCGATGTCGAC	22	5′ RACE; inner
Primer 5	GTGCCAGGTACTTCTCCAGGTACC	24	5′ RACE; inner
Primer 6	AAGCAGTGGTATCAACGCAGAGTAC(T)30VN	57	cDNA synthesis
Primer 7	CTAATACGACTCACTATAGGGCAAGCAGTGGTATCAACCAGA GT (0.4 μM); CTAATACGACTCACTATAGGGC (0.2 μM)	20	3′ RACE
Primer 8	AATGCCCCACAAGTGTTACCA	21	3′ RACE
Primer 9	TCTGGTTTCAGTAATTCGCC	20	Amplification of ORF
Primer 10	TCATGCCATAAATTCATAAGGA	22	Amplification of ORF
Primer 11	GCTCTAGAGCGCCACCATGACAAACACGAAGGGAAAGAG	39	Amplification of ORF
Primer 12	TGTACATCACTTATCGTCGTCATCCTTGTAATCTGCCATGAATTC ATAAGGAATGGGT	58	Amplification of ORF
Primer 13	GCTGGTGCTACGTATGTTGTG	21	Real-time PCR for GAPDH
Primer 14	CAGAGATGATGACCCTCTTGG	21	Real-time PCR for GAPDH
Primer 15	AATGCCCCACAAGTGTTACCA	21	Real-time PCR for *RPL21*
Primer 16	CAGTTCAGGCTCCTTTCCGTT	21	Real-time PCR for *RPL21*
shRNA-F	CCGGAATGCCCCACAAGTGTTACCACTCGAGTGGTAACACTTG TGGGGCATTTTTTTG	58	Knockdown
shRNA-R	AATTCAAAAAAATGCCCCACAAGTGTTACCACTCGAGTGGTAA CACTTGTGGGGCATT	58	Knockdown

V = A, C or G. N = A, C, G, or T. RACE, rapid amplification of cDNA ends; ORF, open reading frame; PCR, polymerase chain reaction; GAPDH, glyceraldehyde 3-phosphate dehydrogenase; *RPL21*, ribosomal protein L21.

datasets [32]. The annotation information and experimental method for the human samples have been previously reported [32]. The relative expression level of *RPL21* in each human tissue was normalized by that in kidney.

Subcloning of porcine *RPL21* coding DNA sequence

The coding DNA sequence (CDS) region of *RPL21* was amplified from the cloned vector mentioned above. We used primers 9 and 10 for the first PCR and the reaction was performed as follows: 94°C initial denaturation for 3 min, 35 cycles of 94°C for 30 sec, 65°C for 30 sec, and 72°C for 1 min, followed by a final extension at 72°C for 5 min. The second PCR amplification was performed using the following schedule: 94°C for 3 min, followed by 35 cycles of 30 sec at 94°C, 60°C for 30 sec, and 72°C for 1 min, followed by a final extension for 5 min at 72°C with primers 11 and 12. The amplified *RPL21* CDS with an *XbaI* site and a Kozak sequence at the 5′ end and a *BsrGI* site and a FLAG tag at the 3′ end was cloned into a TA vector. After sequencing, the newly cloned *RPL21* CDS region was digested with *XbaI* and *BsrGI* from the cloned TA vector and inserted into the corresponding site in the pCAGGS-EGFP-puro vector (Addgene, USA) to construct the pCX-RPL21 vector.

Real-time PCR

The real-time PCR primers for the *RPL21* gene (primers 15 and 16; Table 1) were designed according to the mRNA sequences cloned in this study. The cDNAs were synthesized from total RNA that was extracted from 7 different tissues (kidney, heart, liver, lung, ovary, intestine, and skin) and 3 types of cell lines (wild-type fibroblast, transient *RPL21*-overexpressed fibroblast, and *RPL21*-knockdown fibroblast) by using the TOPscript Reverse Transcriptase kit (Enzynomics, Korea). The *RPL21* expression levels of the different pig tissues were compared by using a standard curve method as previously described [19]. Briefly, a standard curve was constructed with serial ten-fold dilutions of the pCX-RPL21 plasmid DNA by performing real-time PCR. Then the cycle threshold (Ct) value that was obtained from each sample was transformed into a copy number according to the standard curve. The PCR was performed with primers 15 and 16 by using the TOPreal One-step RT qPCR Kit (Enzynomics) with the following conditions: 40 cycles of 10 sec denaturation at 95°C, 15 sec annealing at 64°C with a 0.1°C decrease in each cycle for 30 cycles, and a 20 sec extension at 72°C. When comparing the *RPL21* expression levels in the same tissue or cell line, we normalized the expression level against a housekeeping gene, *GAPDH* (primers 13 and 14).

Cell culture and transient transfection

A porcine ear skin fibroblast (PEF) cell line was isolated from a 10-day-old Messachusetts General Hospital pig [18] and maintained in Dulbecco's Modified Eagle's Medium (Welgene, Korea) supplemented with 20% fetal bovine serum (Gibco, USA), 100 units/mL of penicillin and 100 μg/mL of streptomycin (Gibco), 1× non- essential amino acids (Gibco), 55 μM β-mercaptoethanol (Gibco), and 1 mM sodium pyruvate (Gibco) at 37°C in humidified air containing 5% CO2. The cells were fed every two days and transiently transfected with the constructed plasmid DNA by using Lipofectamine LTX (Invitrogen) according to the manufacturer's protocol. The cells were incubated for an additional 48 h after transfection and then harvested for downstream experiments.

Lentiviral vector construction and infection

A lentiviral vector for targeting exon 4 of pig *RPL21* was constructed according to the Addgene plasmid 10878 protocol. Briefly, we synthesized a sense oligo (shRNA-F) with an *AgeI* site and an antisense oligo (shRNA-R) with an *EcoRI* site for targeting the pig *RPL21* gene (NeoProbe, Korea). After annealing, the hairpin oligo was cloned into an *AgeI*/*EcoRI* double digested lentiviral vector (pLKO.1 TRC). The plasmids carrying the correct insert were screened out and sequenced. Lentiviral particles were produced by packaging the constructed shRNA vector with the psPAX2 and pMD2.G vectors in LentiX-293T cells. PEF cells were then infected with lentiviral particles for 24 h in the presence of 8 μg/mL Polybrene (Sigma-Aldrich, USA). Three days later, cells were harvested for quantitative PCR, western blotting, cell viability assays, and cell cycle assays. The empty pLKO.1 TRC vector containing a fragment of scrambled sequences was used as a negative control.

Immunofluorescent cytochemical (ICC) staining

ICC staining was performed to determine whether the tagged-RPL21 protein was functionally expressed in PEF cells. Briefly, 48 h after transfection, cells were fixed with 4% paraformaldehyde (Sigma-Aldrich) for 15 min at room temperature and permeabilized with 0.25% Triton X-100 (Promega, USA) in Dulbecco's Phosphate-Buffered Saline (DPBS; Welgene) for 15 min. Subsequently, cells were blocked with 1× blocking solution for 1 h at room temperature and incubated with a monoclonal anti-FLAG M2 primary antibody (Sigma-Aldrich) at 4°C in 1× blocking solution overnight. After washing three times with DPBS containing 0.1% (v/v) Tween 20 (PBST; LPS Solution, Korea), the cells were incubated with Alexa Fluor 488 goat anti-mouse IgG (Invitrogen) secondary antibody for 2 h at room temperature followed by incubation for 5 min in 5 μg/mL Hoechst 33342 solution (Sigma-Aldrich). Cell images were captured by using an Axiovert 200M system (Carl Zeiss Light Microscopy, Germany).

Western blot

Transfected PEF cells were harvested by using a cell scraper after washing two times with DPBS. Harvested cells were lysed

by sonication in RIPA lysis buffer (Biosesang, Korea) supplemented with protease inhibitor (Roche Applied Science) and centrifuged at 16,000 × g for 5 min at 4°C to remove cell debris. Protein concentration was determined by using a BCA Protein Assay Kit (Bio-Rad Laboratories, USA). Equal amounts (80 μg) of protein were separated by using a 12% SDS-PAGE gel and then transferred to a polyvinylidene difluoride membrane (No. GF10600023; Millipore, Germany). Subsequently, the membranes were incubated separately with mouse anti-FLAG M2 primary antibody, rabbit anti-β-actin (13E5) monoclonal antibody (Cell Signaling Technology, USA), and rabbit anti-p53 polyclonal antibody or rabbit anti-p21 (Abcam, UK) polyclonal antibody (Abcam) overnight at 4°C. After washing three times with 1× Tris-buffered saline with Tween 20 (LPS Solution), the membranes were incubated with horseradish peroxidase-labeled secondary antibody (Santa Cruz Biotechnology, USA). Chemiluminescent detection was performed by using the ECL reagent (GE Healthcare Life Sciences, USA) and a luminescent image analyzer system (LAS-3000; Fujifilm, Japan).

Cell viability assay and cell cycle analysis

PEF cells that were infected with shRNA vectors for 3 days were used for cell viability and cell cycle assays. Viability assays were performed by using the EZ-CYTOX Cell Viability Assay Kit (DaeilLab Service, Korea) according to the manufacturer's protocol. Cell cycle phases were analyzed by using propidium iodide DNA staining and a flow cytometer equipped with the BD CellQuest Pro Software (BD Bioscience, USA). Briefly, PEF cells were dissociated with 0.25% Trypsin-EDTA (Gibco). The obtained cells were fixed with cold DPBS supplemented with 70% ethanol for 1 h on ice, followed by a single washing with cold DPBS, and incubation with 10 mg/ml RNase A for 1 h (Invitrogen). Finally, the DNA was stained with 1 mg/mL propidium iodide at 4°C until analysis.

Statistical analysis

The relative quantitative PCR data were processed by applying the $2^{-\Delta\Delta Ct}$ method with *GAPDH* as an internal control. Statistical significance was analyzed by using SPSS software (ver. 17.0, SPSS, USA). Data are presented as mean ± SEM values. Statistical significance is indicated by $p < 0.05$ (*) or $p < 0.01$ (**).

Results

Cloning and identification of the pig *RPL21* gene

The full-length cDNA of the porcine *RPL21* gene was cloned and identified in this study (GenBank accession No. KU891824). The porcine *RPL21* gene is located on the "+" strand of chromosome 11 and spans 2167 bp from 4199792 to 4201958. It includes five exons (panel A in Fig. 1) that are 150 bp, 62 bp, 113 bp, 151 bp, and 128 bp in length. The corresponding introns behind each exon are 148 bp, 369 bp, 934 bp, and 114 bp in length, respectively. There are many termination codons that are found at intervals within the cloned sequences, but only one ORF of 483 bp in length that codes for 160 amino acids was identified. An "AAA (ATG) A" context and a typical "TTTTCT" oligopyrimidine tract was identified in the 83 bp 5′ noncoding region, where the pyrimidine residues accounted for up to 58% of the total sequences. With regard to the 38 bp 3′ noncoding region, as expected, an "AATAAA" cleavage-polyadenylation site was identified (panel B in Fig. 1).

Homology analysis and annotation of pig *RPL21* amino acid

Amino acid sequences of the *RPL21* protein from human, mouse, dog, cattle, rat, and zebrafish were aligned with our cloned pig *RPL21*. We found that the pig protein had a completely identical sequence with that of human and dog. Moreover, there was only 1 amino acid difference from that in the mouse sequence and 2 amino acids difference from the cattle and rat sequences (panel A in Fig. 2). Pig *RPL21* shares 99.38% (159/160), 98.75% (158/160), and 98.75% (158/160) sequence similarity with the *RPL21* of mouse, cattle, and rat, respectively. Even in the comparison with zebrafish, which is on a different branch of the evolutionary tree, pig had an approximately 85% (136/160) homology (panel B in Fig. 2).

In addition, conservation of the *RPL21* N-terminal region is much higher than that in its C- terminal region. Given this, we checked the features in the vicinity of the pig *RPL21* terminal region. We observed an SH3-like barrel topology structure in the amino acid sequence from 1 to 100 and an N-glycosylation site from 66 to 69 (shown in bold-red font in panel B in Fig. 1) at a probability of 76.3%. In addition, in porcine *RPL21*, there was a conserved β-strand, similar to that in archaeal RPL21e, and an extension unique to eukaryotes (panel C in Fig. 1).

To clarify the phylogenetic location of pig *RPL21*, a phylogenetic tree was constructed based on the amino acid sequences from 13 other species. As shown in panel B in Fig. 2, pig *RPL21* was positioned on a branch of the mammalian sub-cluster and was most similar to that from human and dog (panel B in Fig. 2). The 1vx4.1.T modeler in the SWISS-MODEL template library was used as a template to predict the spatial structure of pig *RPL21* because it had 99.38% (159/160 amino acids) similarity to our cloned sequences. As shown in panel B in Fig. 1, in total, nine strands and two helices were identified in the secondary structure of pig *RPL21*.

RPL21 is expressed widely in porcine tissues

Real-time quantitative PCR was performed to determine the expression patterns of *RPL21* in various porcine tissues. A standard curve was constructed with serial ten-fold dilutions of the pCX-RPL21 plasmid DNA. As a result, a slope value of −3.2789 and a *r*-squared value of 0.9945 were derived; results that indicate that the efficiency of the amplification reaction

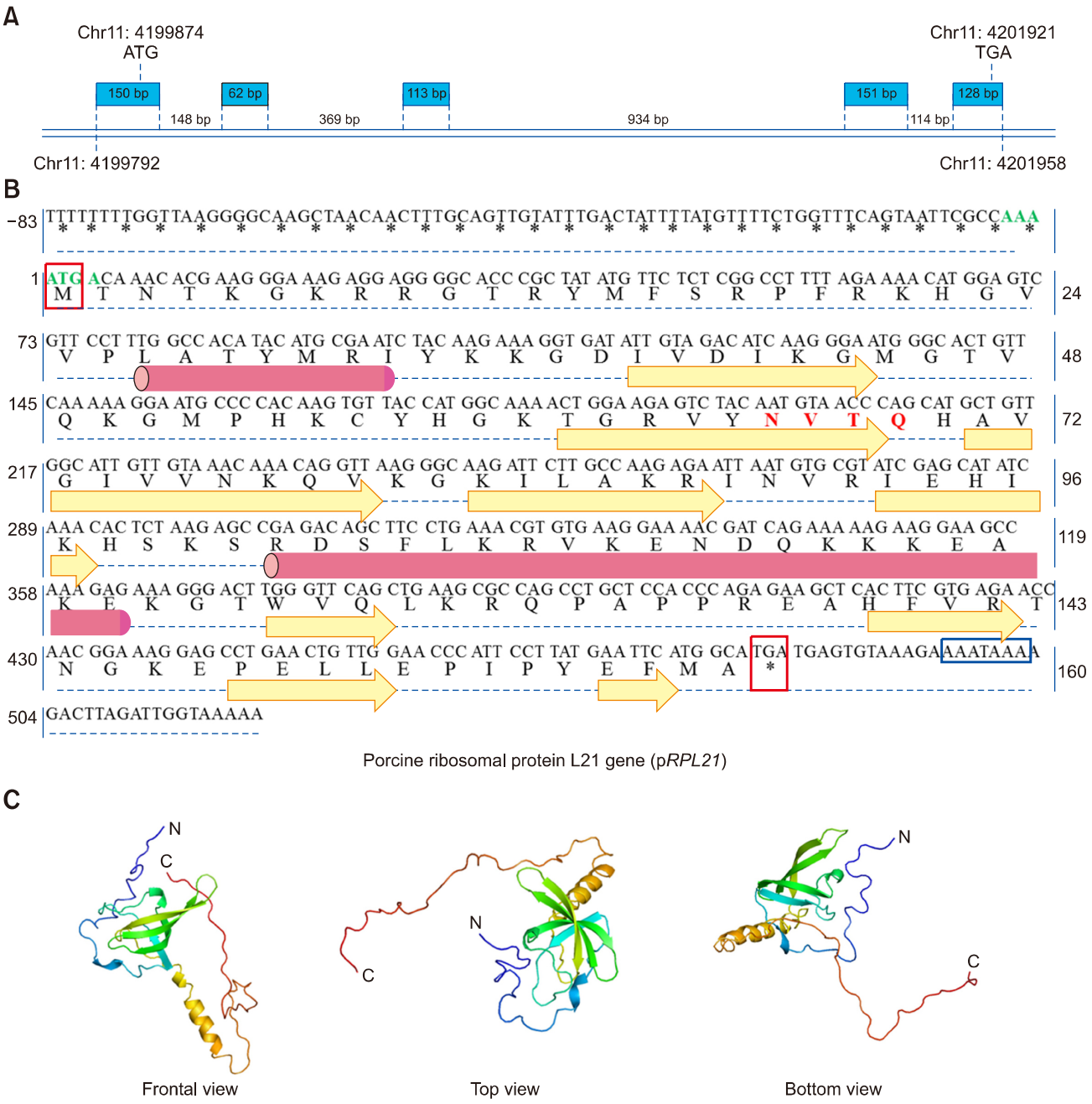

Fig. 1. Sequence analysis of the porcine ribosomal protein L21 (*RPL21*) gene and its inferred amino acid sequence. (A) The schematic representation of the porcine *RPL21* gene mapped to chromosome 11. Blue boxes represent the gene's five exons; there are four intron regions between the exons. (B) Nucleotides and the inferred amino acid sequence of the pig *RPL21* gene. Pink cylinders are helices, and yellow rectangles with an arrow represent strands in the deduced secondary structure. Blue lines represent coils. The start codon and stop codon are indicated by red boxes. A possible N-glycosylation site is shown in red letters. Sequences before the ATG refer to the noncoding region. The "A" in the initiation codon "ATG" is taken as +1. Numbers on the right side of panel B represent the deduced amino acid sequence. (C) The predicted three-dimensional structure of the pig *RPL21* protein. Positions of the N and C termini are shown in capital letters.

was 101.84% and that the amount of product doubles in each cycle (panel A in Fig. 3). On this basis, we performed qPCR with an equivalent template cDNA and found that the pig *RPL21* gene is predominantly expressed in the ovary and lung, with less expression in kidney, small intestine, and skin, and the lowest expression levels in heart and liver (panel A in Fig. 3).

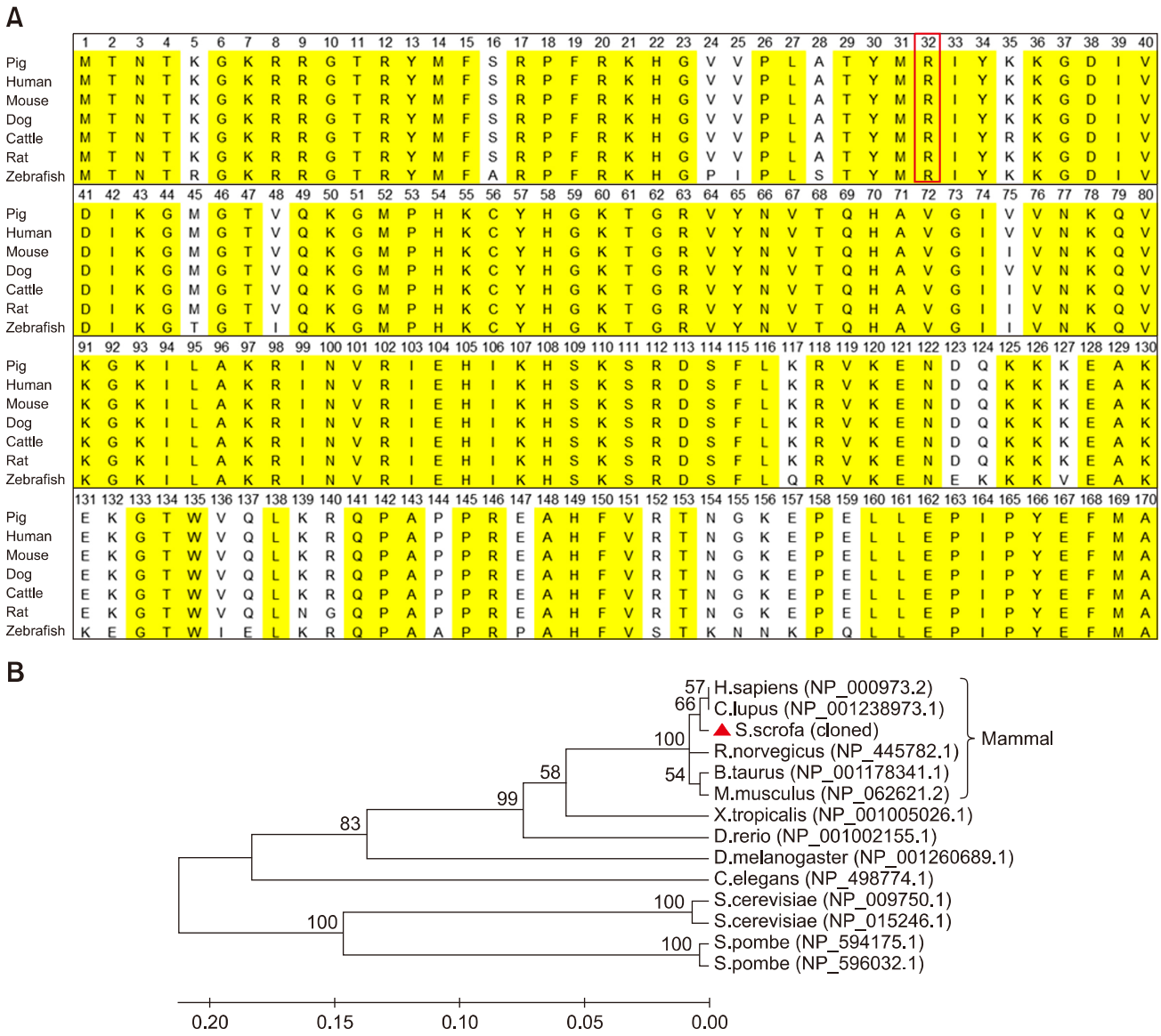

Fig. 2. Conservation and phylogenetic analysis of pig ribosomal protein L21 (RPL21) protein. (A) Multiple sequence alignment of the *RPL21* amino acid sequences across various species. In total, twenty conserved regions were identified and are indicated by yellow shading. The mutation site reported to cause hypotrichosis simplex is indicated with a red box. (B) Phylogenetic analysis of porcine *RPL21* protein with its 12 homologous counterparts has been published previously (accession Nos. in National Center for Biotechnology Information are presented in brackets). Pig, dog, human, mouse, cattle, and rat share more than 95% identity at the amino acid level. The 13 species are *Sus scrofa* (S.scrofa); *Mus musculus* (M.musculus); *Bos taurus* (B.taurus); *Canis lupus familiaris* (C.lupus); *Rattus norvegicus* (R.norvegicus); *Danio rerio* (D.rerio); *Homo sapiens* (H.sapiens); *Xenopus tropicalis* (X.tropicalis); *Drosophila melanogaster* (D.melanogaster); *Caenorhabditis elegans* (C.elegans); *Saccharomyces cerevisiae* S288c (S.cerevisiae), and *Schizosaccharomyces pombe* 972h (S.pombe).

This expression pattern is generally consistent with that reported in human-based study (panel C in Fig. 3).

Overexpression of pig *RPL21* in PEF

To confirm the predicted protein functionality, we inserted the CDS region of the pig *RPL21* gene into a eukaryotic expression vector, pCAGGS-EGFP-Puro (panel A in Fig. 4). Two days after transfection, the expression level of *RPL21* mRNA was significantly up-regulated ($p < 0.05$), more than 8-fold (panel B in Fig. 4), and a protein with molecular weight of approximately 18.5 kDa was detected in the western blot results from transfected cells. This result is consistent with that predicted by our assessment of cloned sequences (panel C in Fig. 4). In addition, we found a fluorescence signal of the

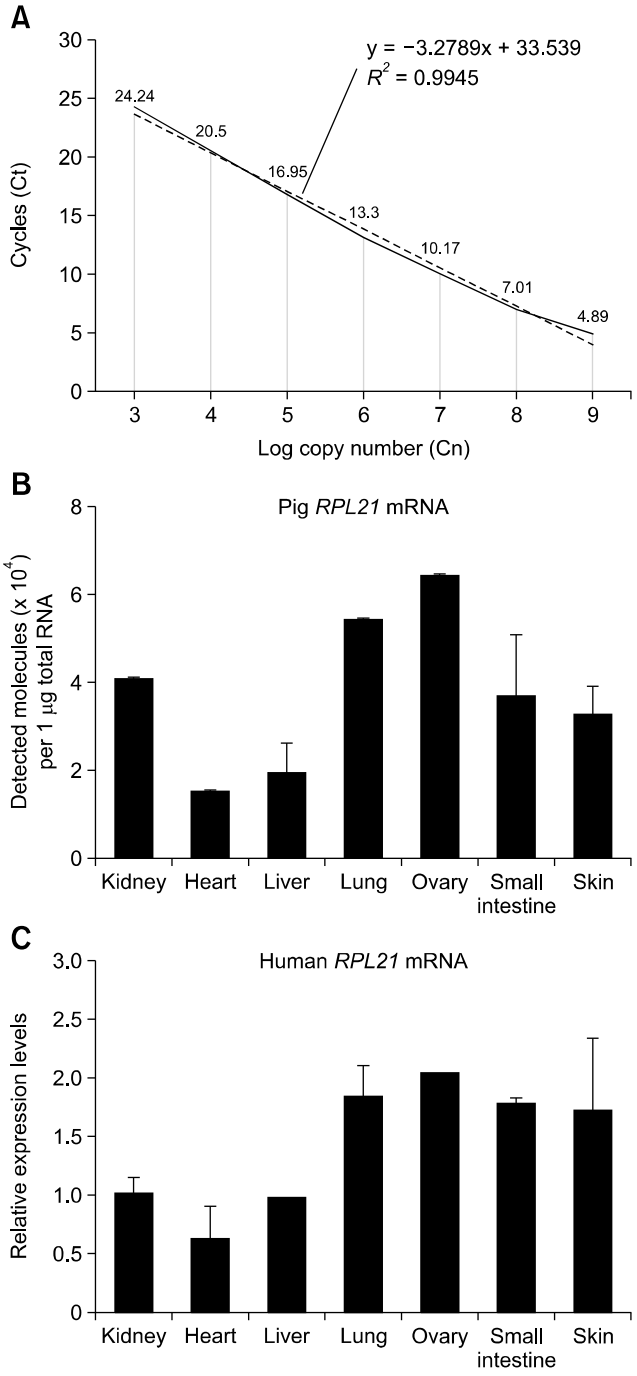

Fig. 3. The expression pattern of the ribosomal protein L21 (*RPL21*) gene in different tissues. (A) A standard curve was constructed with serial ten-fold dilutions of the pCX-RPL21 plasmid DNA by quantitative polymerase chain reaction. (B) The transcript abundance level of *RPL21* mRNA in 7 pig tissues. *RPL21* is relatively highly expressed in ovary and lung, less so in kidney, small intestine, and skin, and expressed at the lowest level in heart and liver. With the exception of kidney, this expression pattern is similar to that in human tissues (C). Data are presented as mean ± SEM values. Similar results were observed in more than two independent experiments.

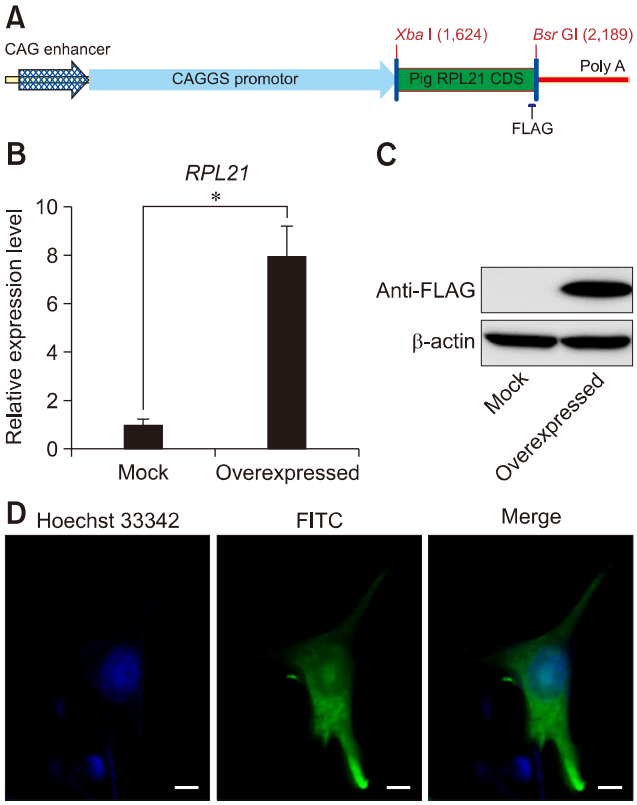

Fig. 4. Overexpression of pig ribosomal protein L21 (RPL21) in a pig fibroblast cell line. (A) Schematic diagram of the vector used for *RPL21* overexpression. (B) There was more than an 8-fold change in the expression level of *RPL21* mRNA after transfection with pCX-RPL21 vector. (C) The deduced protein with a molecular weight of approximately 18.5 kDa was confirmed by western blotting. (D) Pig *RPL21* localized to both cytoplasm and nuclei as detected by double immunofluorescence staining. Beta-actin was used as an internal control for the western blot analysis. Glyceraldehyde 3-phosphate dehydrogenase was used as an internal control for the real-time polymerase chain reaction. Data are presented as mean ± SEM values. *$p < 0.05$ *vs*. normal. Similar results were observed in more than two independent experiments. Scale bars = 10 μm.

FLAG-tagged *RPL21* protein in both the cytoplasm and nuclei (panel D in Fig. 4).

Knockdown of *RPL21* affects cell proliferation and cell cycle

To assess the effect of *RPL21* down-regulation on cell growth, a vector that expressed shRNAs was infected into PEF cells. After transduction, the shRNA vector produced a significant decrease in the level of *RPL21* expression (panel A in Fig. 5). More importantly, cell proliferation activity was significantly decreased ($p < 0.01$), by nearly 36%, in the knockdown group compared to those in wild-type PEF cells and PEF cells transfected with an empty pLKO.1 vector (panel B in Fig. 5). Hence, we checked the expression levels of 6 proteins

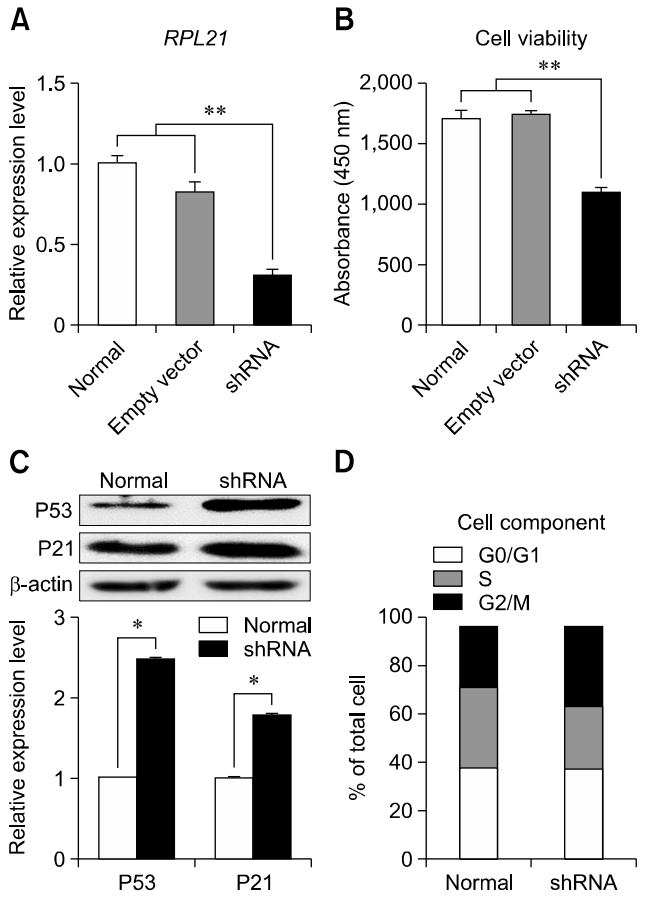

Fig. 5. Knockdown of ribosomal protein L21 (*RPL21*) may inhibit the proliferation of porcine ear skin fibroblast (PEF) cells and induce cell cycle arrest. (A) Real-time polymerase chain reaction (PCR) results show a significant decrease in the level of *RPL21* expression following RNA interference. (B) Knockdown of *RPL21* significantly inhibited the proliferation of PEF cells. (C) The expression levels of p53 and p21 protein were investigated by western blotting. (D) Knockdown of *RPL21* led to G2 arrest. Beta-actin was used as an internal control in the western blotting. Glyceraldehyde 3-phosphate dehydrogenase was used as an internal control for real-time PCR. Data are presented as mean ± SEM values. $*p < 0.05$, $**p < 0.01$ *vs*. normal. Similar results were observed in more than two independent experiments.

that are related to the cell cycle and apoptosis. The results showed that the expression of p53 and p21 significantly increased ($p < 0.05$) (panel C in Fig. 5), but the caspase-3, cytochrome c, bax, and bcl-2 expression levels were unaffected (data not shown). To determine whether knockdown of *RPL21* inhibited cell proliferation by influencing the cell cycle distribution pattern, the DNA content from wild-type PEF cells and lentiviral vector-infected PEF cells was analyzed. The results demonstrated that knockdown of *RPL21* induces an obvious depletion of cells at the G0/G1 and S phases with a simultaneous accumulation of cells at the G2/M phase (panel D in Fig. 5).

Discussion

The mRNA and amino acid sequences of *RPL21* in several species have been previously reported [20,29]. However, there has been little reported on the pig *RPL21* gene prior to this study. Herein, we report on our analysis of cloned sequences, the results of which showed that pig *RPL21* has many typical features in both its mRNA and amino acid sequences. For example, we found that pig *RPL21* mRNA consists of 5 exons, which is similar to that of the human gene [9]. However, pig *RPL21* does not have the common Kozak sequence around the translation initiation site, a sequence that is thought to be important in the initiation of the translation process and always occurs in eukaryotic mRNAs [6,17]. Instead, pig, human, and rat share the same "AAAATGA" context, rather than the common "ACCATGG" in other species [9,17]. Many eukaryotic RP mRNAs are rich in pyrimidine residues in their 5′ UTR region, which is a common feature in other well-characterized RPs that play important roles in regulating transcription [8,24]. Therefore, we scanned the 5′ UTR region of pig *RPL21* and found a "TTTTCT" oligopyrimidine tract, as expected. In addition to mRNA sequences, RPs appear to be well-conserved throughout evolution [37]. Thus, we analyzed pig *RPL21* amino acid structure and observed an SH3-like domain in pig *RPL21*, which may indicate that pig *RPL21* is an SH3 domain-containing protein, as has been reported for *RPL6*, *RPL14*, and *RPL16* [15].

Most ribosomal genes can be considered housekeeping genes because of their breadth of expression in almost all cell types [12,25]. However, there are a few exceptions, such as the *RPL19* [28], RPL3-like, and RPL39-like genes that are only expressed in a few tissues [35]. In this study, all 6 pig tissues showed detectable levels of *RPL21* expression. Similar to *RPL21* expression distribution in human tissues [35], the highest level of *RPL21* expression in pig was in ovary. This may be because a high level of metabolism or protein synthesis is needed in ovary tissue.

Next, we studied the localization of pig *RPL21* and found it was localized in both cytoplasm and nuclei, as has been reported for *RPL5* [30]. However, our result is different from that for human *RPL21*, which is mainly localized in cytoplasm. There are three major potential causes of this difference: first, we used a FLAG oligomeric peptide to tag the *RPL21* protein instead of using the *RPL21* antibody directly; this may have led to a change in the normal localization pattern of the protein [31], second, many RPs need to be transported into the nucleus after their synthesis in the cytoplasm [26], and third, because an overabundance of tagged proteins is produced by overexpression, they may fail to incorporate into ribosomes and may become scattered across the nuclear region.

RPs have important roles in the process of cell growth. The abnormal expression of RPs can cause defective ribosome

biogenesis and trigger ribosomal stress (also termed nucleolar stress), leading to p53-dependent cell cycle arrest or apoptosis [4,11]. Generally, an increased expression of p53 and p21 has been observed in cells that arrest at the G1 phase; however, in some cases, the induction of G2 arrest by p53 and p21 also has been reported [1,34]. In this study, knockdown of pig *RPL21* induced an obvious accumulation of cells at the G2/M phase with a simultaneous up-regulation of p53 and p21. This likely due to knockdown of *RPL21* affecting normal ribosome assembly. The unassembled RPs subsequently relocate from the nucleolus to the nucleoplasm where they can bind to Mdm2 and activate the expression of p53, p21, and other responsive factors that related to cell cycle arrest [7,45]. Certainly, the detailed regulatory mechanism between the p53 signaling pathway and RPs is very complex [36], and further research is needed.

Many fundamental investigations into pig *RPL21* were included in this study, such as assessment of *RPL21* conservation, sequence signature, spatial structure, expression pattern, and protein localization, among others. Although we did not perform a systematic study into the molecular mechanisms involved in pig *RPL21* function, we did observe that the *RPL21* expression level is closely associated with cell proliferation and cell cycle arrest. We anticipate that the results of this study may provide a basis for further study of the pig *RPL21* gene and hypotrichosis simplex.

Acknowledgments

This work was carried out with the support of Next Generation Biogreen 21 (project No. PJ0110412016) of the Rural Development Administration and funded by the KRIBB Research Initiative Program, Republic of Korea.

Conflict of Interest

The authors declare no conflicts of interest.

References

1. **Agarwal ML, Agarwal A, Taylor WR, Stark GR.** p53 controls both the G2/M and the G1 cell cycle checkpoints and mediates reversible growth arrest in human fibroblasts. Proc Natl Acad Sci U S A 1995, **92**, 8493-8497.
2. **Artimo P, Jonnalagedda M, Arnold K, Baratin D, Csardi G, de Castro E, Duvaud S, Flegel V, Fortier A, Gasteiger E, Grosdidier A, Hernandez C, Ioannidis V, Kuznetsov D, Liechti R, Moretti S, Mostaguir K, Redaschi N, Rossier G, Xenarios I, Stockinger H.** ExPASy: SIB bioinformatics resource portal. Nucleic Acids Res 2012, **40**, W597-603.
3. **Bhavsar RB, Makley LN, Tsonis PA.** The other lives of ribosomal proteins. Hum Genomics 2010, **4**, 327-344.
4. **Chakraborty A, Uechi T, Kenmochi N.** Guarding the 'translation apparatus': defective ribosome biogenesis and the p53 signaling pathway. Wiley Interdiscip Rev RNA 2011, **2**, 507-522.
5. **Chenna R, Sugawara H, Koike T, Lopez R, Gibson TJ, Higgins DG, Thompson JD.** Multiple sequence alignment with the Clustal series of programs. Nucleic Acids Res 2003, **31**, 3497-3500.
6. **De Angioletti M, Lacerra G, Sabato V, Carestia C.** β+45 G → C: a novel silent β-thalassaemia mutation, the first in the Kozak sequence. Br J Haematol 2004, **124**, 224-231.
7. **Deisenroth C, Zhang Y.** The ribosomal protein-Mdm2-p53 pathway and energy metabolism: bridging the gap between feast and famine. Genes Cancer 2011, **2**, 392-403.
8. **Devi KRG, Chan YL, Wool IG.** The primary structure of rat ribosomal protein S4. Biochim Biophys Acta 1989, **1008**, 258-262.
9. **Frigerio JM, Dagorn JC, Iovanna JL.** Cloning, sequencing and expression of the L5, L21, L27a, L28, S5, S9, S10 and S29 human ribosomal protein mRNAs. Biochim Biophys Acta 1995, **1262**, 64-68.
10. **Harms J, Schluenzen F, Zarivach R, Bashan A, Gat S, Agmon I, Bartels H, Franceschi F, Yonath A.** High resolution structure of the large ribosomal subunit from a mesophilic eubacterium. Cell 2001, **107**, 679-688.
11. **Hou YL, Ding X, Hou W, Song B, Wang T, Wang F, Li J, Zhong J, Xu T, Ma BX, Zhu HQ, Li JH, Zhong JC.** Overexpression, purification, and pharmacologic evaluation of anticancer activity of ribosomal protein L24 from the giant panda (*Ailuropoda melanoleuca*). Genet Mol Res 2013, **12**, 4735-4750.
12. **Hsiao LL, Dangond F, Yoshida T, Hong R, Jensen RV, Misra J, Dillon W, Lee KF, Clark KE, Haverty P, Weng Z, Mutter GL, Frosch MP, MacDonald ME, Milford EL, Crum CP, Bueno R, Pratt RE, Mahadevappa M, Warrington JA, Stephanopoulos G, Stephanopoulos G, Gullans SR.** A compendium of gene expression in normal human tissues. Physiol Genomics 2001, **7**, 97-104.
13. **Jones P, Binns D, Chang HY, Fraser M, Li W, McAnulla C, McWilliam H, Maslen J, Mitchell A, Nuka G.** InterProScan 5: genome-scale protein function classification. Bioinformatics 2014, **30**, 1236-1240.
14. **Kiefer F, Arnold K, Künzli M, Bordoli L, Schwede T.** The SWISS-Model Repository and associated resources. Nucleic Acids Res 2009, **37**, D387-392.
15. **Klinge S, Voigts-Hoffmann F, Leibundgut M, Arpagaus S, Ban N.** Crystal structure of the eukaryotic 60S ribosomal subunit in complex with initiation factor 6. Science 2011, **334**, 941-948.
16. **Korobeinikova AV, Garber MB, Gongadze GM.** Ribosomal proteins: structure, function, and evolution. Biochemistry (Mosc) 2012, **77**, 562-574.
17. **Kozak M.** Point mutations define a sequence flanking the AUG initiator codon that modulates translation by eukaryotic ribosomes. Cell 1986, **44**, 283-292.
18. **Kwon DJ, Jeon H, Oh KB, Ock SA, Im GS, Lee SS, Im SK, Lee JW, Oh SJ, Park JK, Hwang S.** Generation of leukemia inhibitory factor-dependent induced pluripotent stem cells from the Massachusetts General Hospital miniature pig. Biomed Res Int 2013, **2013**, 140639.
19. **Lee C, Kim J, Shin SG, Hwang S.** Absolute and relative QPCR quantification of plasmid copy number in *Escherichia*

coli. J Biotechnol 2006, **123**, 273-280.
20. **Lin A, Chan YL, Jones R, Wool IG.** The primary structure of rat ribosomal protein S12. The relationship of rat S12 to other ribosomal proteins and a correlation of the amino acid sequences of rat and yeast ribosomal proteins. J Biol Chem 1987, **262**, 14343-14351.
21. **Lindström MS.** Emerging functions of ribosomal proteins in gene-specific transcription and translation. Biochem Biophys Res Commun 2009, **379**, 167-170.
22. **Liu JM, Ellis SR.** Ribosomes and marrow failure: coincidental association or molecular paradigm? Blood 2006, **107**, 4583-4588.
23. **Loreni F, Francesconi A, Jappelli R, Amaldi F.** Analysis of mRNAs under translational control during Xenopus embryogenesis: isolation of new ribosomal protein clones. Nucleic Acids Res 1992, **20**, 1859-1863.
24. **Loreni F, Ruberti I, Bozzoni I, Pierandrei-Amaldi P, Amaldi F.** Nucleotide sequence of the L1 ribosomal protein gene of *Xenopus laevis*: remarkable sequence homology among introns. EMBO J 1985, **4**, 3483-3488.
25. **Nygard AB, Jørgensen CB, Cirera S, Fredholm M.** Selection of reference genes for gene expression studies in pig tissues using SYBR green qPCR. BMC Mol Biol 2007, **8**, 67.
26. **Plafker SM, Macara IG.** Ribosomal protein L12 uses a distinct nuclear import pathway mediated by importin 11. Mol Cell Biol 2002, **22**, 1266-1275.
27. **Plaks V, Gershon E, Zeisel A, Jacob-Hirsch J, Neeman M, Winterhager E, Rechavi G, Domany E, Dekel N.** Blastocyst implantation failure relates to impaired translational machinery gene expression. Reproduction 2014, **148**, 87-98.
28. **Rebouças EL, Costa JJN, Passos MJ, Passos JRS, van den Hurk R, Silva JRV.** Real time PCR and importance of housekeepings genes for normalization and quantification of mRNA expression in different tissues. Braz Arch Biol Technol 2013, **56**, 143-154.
29. **Rosendahl G, Andreasen PH, Kristiansen K.** Structure and evolution of the *Tetrahymena thermophila* gene encoding ribosomal protein L21. Gene 1991, **98**, 161-167.
30. **Rosorius O, Fries B, Stauber RH, Hirschmann N, Bevec D, Hauber J.** Human ribosomal protein L5 contains defined nuclear localization and export signals. J Biol Chem 2000, **275**, 12061-12068.
31. **Snapp E.** Design and use of fluorescent fusion proteins in cell biology. Curr Protoc Cell Biol 2005, **Suppl 27**, Unit 21.4.
32. **Su AI, Wiltshire T, Batalov S, Lapp H, Ching KA, Block D, Zhang J, Soden R, Hayakawa M, Kreiman G, Cooke MP, Walker JR, Hogenesch JB.** A gene atlas of the mouse and human protein-encoding transcriptomes. Proc Natl Acad Sci U S A 2004, **101**, 6062-6067.
33. **Tamura K, Peterson D, Peterson N, Stecher G, Nei M, Kumar S.** MEGA5: Molecular Evolutionary Genetics Analysis using maximum likelihood, evolutionary distance, and maximum parsimony methods. Mol Biol Evol 2011, **28**, 2731-2739.
34. **Taylor WR, Stark GR.** Regulation of the G2/M transition by p53. Oncogene 2001, **20**, 1803-1815.
35. **Thorrez L, Van Deun K, Tranchevent LC, Van Lommel L, Engelen K, Marchal K, Moreau Y, Van Mechelen I, Schuit F.** Using ribosomal protein genes as reference: a tale of caution. PLoS One 2008, **3**, e1854.
36. **Wang W, Nag S, Zhang X, Wang MH, Wang H, Zhou J, Zhang R.** Ribosomal proteins and human diseases: pathogenesis, molecular mechanisms, and therapeutic implications. Med Res Rev 2015, **35**, 225-285.
37. **Warner JR.** Synthesis of ribosomes in *Saccharomyces cerevisiae*. Microbiol Rev 1989, **53**, 256-271.
38. **Warner JR, McIntosh KB.** How common are extraribosomal functions of ribosomal proteins? Mol Cell 2009, **34**, 3-11.
39. **Weisberg RA.** Transcription by moonlight: structural basis of an extraribosomal activity of ribosomal protein S10. Mol Cell 2008, **32**, 747-748.
40. **Wool IG.** The structure and function of eukaryotic ribosomes. Annu Rev Biochem 1979, **48**, 719-754.
41. **Wool IG, Chan YL, Glück A.** Structure and evolution of mammalian ribosomal proteins. Biochem Cell Biol 1995, **73**, 933-947.
42. **Xie M, Kobayashi I, Kiyoshima T, Nagata K, Ookuma Y, Fujiwara H, Sakai H.** In situ expression of ribosomal protein L21 in developing tooth germ of the mouse lower first molar. J Mol Histol 2009, **40**, 361-367.
43. **Yusupova G, Yusupov M.** High-resolution structure of the eukaryotic 80S ribosome. Annu Rev Biochem 2014, **83**, 467-486.
44. **Zhang W, Hawse J, Huang Q, Sheets N, Miller KM, Horwitz J, Kantorow M.** Decreased expression of ribosomal proteins in human age-related cataract. Invest Ophthalmol Vis Sci 2002, **43**, 198-204.
45. **Zhang Y, Lu H.** Signaling to p53: ribosomal proteins find their way. Cancer Cell 2009, **16**, 369-377.
46. **Zhou C, Zang D, Jin Y, Wu H, Liu Z, Du J, Zhang J.** Mutation in ribosomal protein L21 underlies hereditary hypotrichosis simplex. Hum Mutat 2011, **32**, 710-714.